Optimal Path Tracking Control of a Quadrotor UAV

Conference Paper · May 2014

DOI: 10.1109/ICUAS.2014.6842246

CITATIONS
32

READS
704

2 authors:

Emre Can Suicmez
Middle East Technical University
6 PUBLICATIONS **47** CITATIONS
SEE PROFILE

Ali Kutay
Middle East Technical University
56 PUBLICATIONS **357** CITATIONS
SEE PROFILE

2014 International Conference on Unmanned Aircraft Systems (ICUAS)
May 27-30, 2014. Orlando, FL, USA

Optimal Path Tracking Control of a Quadrotor UAV

Emre Can Suicmez
Aerospace Engineering
Middle East Technical University
Ankara, TURKEY
Email: esuicmez@ae.metu.edu.tr

Ali Turker Kutay
Aerospace Engineering
Middle East Technical University
Ankara, TURKEY
Email: kutay@metu.edu.tr

***Abstract*—This paper presents the linear quadratic tracking (LQT) control of a quadrotor UAV by solving discrete time matrix difference Riccati Equation. First, the nonlinear dynamic model of the quadrotor is obtained by using Newton's equations of motion. Then, the nonlinear dynamic model is linearized around hover condition. The linearized dynamic model is used to solve the optimal control problem. A trade off between good tracking performance and energy consumption is made while defining the performance index (cost function). Time-variant optimal control gains are found off-line by solving discrete time matrix difference Riccati Equation backwards in time. Finally, to validate optimal control system, simulations are performed by using the nonlinear dynamic model as plant and time-variant optimal control gains as state feedback control. The optimal control algorithm used in this paper uses time-variant control gains instead of fixed (time-invariant) control gains used in classical LQR control. Simulations show that, good tracking performance is achieved while decreasing energy consumption compared to the fixed gain LQR control. Some other advantageous properties of the optimal control system used in this paper compared to the fixed gain LQR control are also analyzed. In addition, disturbance rejection properties of the optimal control system are also studied. All algorithms and simulations are done by using MATLAB software.**

***Index Terms*—Quadrotor UAV, Dicrete Time, Path Tracking, Riccati Equation, Nonlinear Dynamic Model, LQT, LQR, Optimal Control, Energy Consumption, Disturbance Rejection**

I. Introduction

Quadrotor is a very popular UAV (Unmanned Aerial Vehicle) concept since it can perform vertical take-off and landing (VTOL) with simple mechanical structure compared to other VTOL UAVs [4]. It can also perform high maneuverable flight [1]. Therefore, it has very flexible operational capabilities especially for complex indoor environments.

Quadrotors have four rotors, and control of the vehicle can be performed by adjusting the speeds of these rotors properly. However, designing control systems for quadrotors is a challenging task since it is a highly nonlinear, dynamically unstable and underactuated system [4] [10]. In addition, an important drawback of quadrotor is high energy consumption [3]. Therefore, in this paper, an optimal path tracking controller is designed to satisfy good tracking performance while decreasing energy consumption.

Many researchers developed path tracking control algorithms for quadrotors. Nonlinear control methods such as backstepping, adaptive backstepping, feedback linearization and sliding mode control are designed by some researchers [1] [4] [5] [8] [10]. As optimal control systems, classical LQR control systems are used by some researchers [7] [9] [11] [12]. These systems mostly use constant (time-invariant) control gains as state feedback control and focus on stabilizing the quadrotor instead of tracking a desired trajectory. On the other hand, the optimal control system used in this paper can be considered as a more unique control approach since it uses time-variant optimal control gains to follow a desired trajectory. The benefit of the approach is that for aggressive maneuvers that force the quadrotor to depart from equilibrium hover condition, time varying control gains that are optimized for the commanded trajectory are used.

In this paper, an optimal LQT control system is obtained by solving discrete time matrix difference Riccati Equation backwards in time. The discrete-time LQT algorithm (optimal control algorithm) is used to obtain time variant optimal control gains to use in state feedback control [2].

First, the nonlinear dynamic model of quadrotor is obtained by using Newton's equations of motion. The nonlinear dynamic model is used to test the optimal control system by simulations. Then, the nonlinear dynamic model is simplified to use in optimal control algorithm. The simplified nonlinear dynamic model is linearized around a pre-defined hover condition. Then, linearized model is discretized by choosing a realistic and computationally efficient sample time. A simple path to be followed is generated. Path involves a climb, turn and descent. In addition, more complex paths are also generated. Then, the tracking of the desired trajectory is formulated as a discrete time LQT problem [2]. Time-variant optimal control gains are obtained by solving discrete time matrix difference Riccati Equation backwards in time. Time variant optimal control gains that are calculated off-line are used as a state feedback controller to design the optimal control system.

Since a linearized model is used to obtain optimal control gains, states that are related to the trigonometric terms are limited to get more accurate results while verifying the

978-1-4799-2376-2/14/$31.00 ©2014 IEEE

TABLE I
SYMBOLS AND ABBREVIATIONS

Symbol	Definition
ϕ	Roll angle
θ	Pitch angle
ψ	Yaw angle
Euler angles	ϕ,θ,ψ
$[p,q,r]^T$	Body angular rates
$[\dot{\phi},\dot{\theta},\dot{\psi}]^T$	Rate of change of Euler angles
U_1,U_2,U_3,U_4	Control inputs
m	Mass of the quadrotor
I_x,I_y,I_z	Body inertia
g	Gravitational acceleration
d	Level arm
$\dot{f}(\cdot)$	First order time derivative
$\ddot{f}(\cdot)$	Second order time derivative
$I_{n\times n}$	n_{th} order identity matrix
LQR	Linear Quadratic Regulator
LQT	Linear Quadratic Tracking
RHS	Right hand side
LHS	Left hand side
$c(\cdot)$	cosine function
$s(\cdot)$	sine function
N	Newton

optimal controller by simulations in which the nonlinear dynamic model is used as plant. The state and control weight matrices of the performance index are chosen after trial and error to achieve satisfactory performance.

Finally, optimal control system is simulated by using the nonlinear dynamic model and it is seen that simulations give good tracking performance, reduce the energy consumption compared to the fixed gain LQR controller and satisfy the constraints on states and control.

The quadrotor used in this paper is "AscTech Hummingbird" developed by Ascending Technologies and parameters of the "AscTech Hummingbird" is used throughout the paper. [6]

II. DYNAMIC MODEL OF QUADROTOR

Before deriving dynamic model of quadrotor, first, the relation between force, torque generated by rotors and rotational speed of rotors will be explained. Moreover, control inputs will be defined. Then, the nonlinear dynamic model will be derived by using Newton's equations of motion. Finally, the nonlinear dynamic model will be simplified to use in optimal control algorithm.

A. Relation Between Thrust, Torque and Rotational Speed of Rotors

The relation between the thrust, torque generated by rotors and rotational speed of the rotors are found to be quadratic

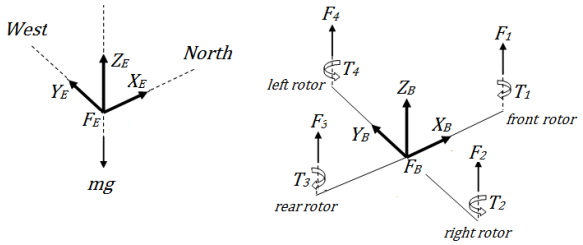

Fig. 1. Reference frames F_B, F_E and force and torque generated by each rotor of the quadrotor.

for AscTech Hummingbird quadrotor [6]. Then, F_i and T_i which are defined in Table II, can be formulated as follows:

$$F_i = \omega_i^2 k_n, \quad for \;\; i = 1,2,3,4 \tag{1}$$
$$T_i = F_i k_m, \quad for \;\; i = 1,2,3,4 \tag{2}$$

Figure 1 also gives visual information about the force and torque generated by each rotor.

B. Defining Control Inputs

Control inputs U_1, U_2, U_3, U_4 are defined as follows:

$$U_1 = F_1 + F_2 + F_3 + F_4 \tag{3}$$
$$U_2 = F_4 - F_2 \tag{4}$$
$$U_3 = F_3 - F_1 \tag{5}$$
$$U_4 = T_2 + T_4 - T_1 - T_3 \tag{6}$$

According to equation (3), U_1 is the total force generated by four rotors. As can be seen in equation (25), U_1 is the driving force to move the quadrotor in x,y and z direction. Therefore, U_1 is directly related to the energy consumption. As mentioned previously, in this paper, one of the aim is optimizing U_1 to decrease energy consumption. Moreover, as can be seen in equation (29), U_2, U_3 and U_4 are related to roll, pitch and yaw motion, respectively.

Actually, Euler angles, ϕ and θ also act as control inputs to control translational motion. By changing angles ϕ and θ, contribution of U_1 in x and y directions change, then the motion in x and y directions occur. By using Euler angles as control inputs the control problem due to underactuated nature of the system can be solved.

C. The Nonlinear Dynamic Model

Before deriving the nonlinear dynamic model, reference frames have to be identified. Two frame of reference will be used in this paper. These are Earth fixed reference frame, F_E and body fixed reference frame, F_B. Earth fixed reference frame is considered as an inertial frame of reference since Earth's rotation relative to distant stars is negligable [13].

TABLE II
SYMBOLS RELATED TO FORCE, TORQUE AND ROTATIONAL SPEED CONVERSION

Symbol	Definition
F_i	Force generated by i_{th} rotor
T_i	Torque generated by i_{th} rotor
ω_i	Angular velocity of i_{th} rotor
k_n	Constant that relates F_i and ω_i
k_m	Constant that relates F_i and T_i

Figure 1 gives detailed information about reference frames, F_E and F_B. F_B is fixed to the quadrotor body and it tranlates and rotates with the body [14].

The position and orientation vector of the quadrotor expressed in the frame F_E relative to fixed origin of F_E can be defined as follows, respectively [10]:

$$\xi = [x, y, z]^T \tag{7}$$
$$\eta = [\phi, \theta, \psi]^T \tag{8}$$

Translational and rotational velocities of F_B relative to our inertial frame of reference F_E are defined as follows, respectively [13]:

$$V_B = [u, v, w]^T \tag{9}$$
$$\omega = [p, q, r]^T \tag{10}$$

In equations (9) and (10), V_B and ω represent the translational and rotational velocities of the quadrotor relative to Earth fixed reference frame F_E, expressed in body fixed reference frame, F_B.

Kinematic equations that relate velocity vectors $(\dot{\xi}, V_B)$ and $(\dot{\eta}, \omega)$ can be expressed as follows [10]:

$$\dot{\xi} = L_{EB} V_B \tag{11}$$
$$\omega = L_R \dot{\eta} \tag{12}$$
$$V_B = L_{BE} \dot{\xi} \tag{13}$$
$$\dot{\eta} = L_R^{-1} \omega \tag{14}$$

where $\dot{\xi}$ and $\dot{\eta}$ are time derivative of ξ and η, respectively. L_{EB} is transformation matrix from F_B to F_E and L_{BE} is transformation matrix from F_E to F_B for translational motion. L_R and L_R^{-1} are transformation matrices for angular velocities. L_{EB}, L_R and L_R^{-1} are defined as follows [13] [15]:

$$L_{EB} = \begin{bmatrix} c(\theta)c(\psi) & s(\phi)s(\theta)c(\psi) - c(\phi)s(\psi) & c(\phi)s(\theta)c(\psi) + s(\phi)s(\psi) \\ c(\theta)s(\psi) & s(\phi)s(\theta)s(\psi) + c(\phi)c(\psi) & c(\phi)s(\theta)s(\psi) - s(\phi)c(\psi) \\ -s(\theta) & s(\phi)c(\theta) & c(\phi)c(\theta) \end{bmatrix} \tag{15}$$

$$L_R = \begin{bmatrix} 1 & 0 & -sin(\theta) \\ 0 & cos(\phi) & sin(\phi)cos(\theta) \\ 0 & -sin(\phi) & cos(\phi)cos(\theta) \end{bmatrix} \tag{16}$$

$$L_R^{-1} = \begin{bmatrix} 1 & sin(\phi)tan(\theta) & cos(\phi)tan(\theta) \\ 0 & cos(\phi) & -sin(\phi) \\ 0 & sin(\phi)/cos(\theta) & cos(\phi)/cos(\theta) \end{bmatrix} \tag{17}$$

By using orthogonality property of transformation matrix L_{EB}, following relations can be obtained [14] [15]:

$$L_{BE} = L_{EB}^{-1} = L_{EB}^T \tag{18}$$
$$\dot{L}_{EB} = L_{EB}\, \tilde{\omega} \tag{19}$$

where:

$$\tilde{\omega} = \begin{bmatrix} 0 & -r & q \\ r & 0 & -p \\ -q & p & 0 \end{bmatrix}, \quad \tilde{\omega} V = \omega \times V \tag{20}$$

Then, Newton's law for translational and rotational motion, written in the reference frame F_B can be obtained as follows, respectively [10]:

$$\sum F_{ext} = m\dot{V}_B + \omega \times (mV_B) \tag{21}$$
$$\sum M_{ext} = J\dot{\omega} + \omega \times (J\omega) \tag{22}$$

where, $\dot{V}_B$ and $\dot{\omega}$ are time derivative of V_B and ω, respectively. The term "$\times$" represents cross product. $\sum F_{ext}$ and $\sum M_{ext}$ in equations (21) and (22), represent the net force and moment acting on the quadrotor, expressed in reference frame F_B, respectively. $\sum F_{ext}$ and $\sum M_{ext}$ are defined as follows:

$$\sum F_{ext} = -L_{BE}\, m \begin{bmatrix} 0 \\ 0 \\ g \end{bmatrix} + \begin{bmatrix} 0 \\ 0 \\ U_1 \end{bmatrix} - K_t V_B \tag{23}$$

$$\sum M_{ext} = \begin{bmatrix} U_2\, d \\ U_3\, d \\ U_4 \end{bmatrix} \tag{24}$$

In equation (23), on the RHS, first term represent gravitational force expressed in F_B, second term is net force generated by rotors and the last term is aerodynamic drag term for translational motion. K_t is a diagonal constant matrix which is taken as $K_t = diag[0.1, 0.1, 0.1]$. In equation (24), on the RHS, there is only one term which represents the net moment generated by rotors.

By replacing equations (23), (24) into equations (21), (22) and by using equations (11), (12),...(20), final form of the nonlinear dynamic model can be obtained as follows:

$$\begin{bmatrix} \ddot{x} \\ \ddot{y} \\ \ddot{z} \end{bmatrix} = -\begin{bmatrix} 0 \\ 0 \\ g \end{bmatrix} + L_{EB} \begin{bmatrix} 0 \\ 0 \\ U_1/m \end{bmatrix} - (K_t/m) \begin{bmatrix} \dot{x} \\ \dot{y} \\ \dot{z} \end{bmatrix} \tag{25}$$

$$\begin{bmatrix}\dot{p}\\ \dot{q}\\ \dot{r}\end{bmatrix} = \begin{bmatrix}(I_y - I_z)qr/I_x\\ (I_z - I_x)pr/I_y\\ (I_x - I_y)pq/I_z\end{bmatrix} + \begin{bmatrix}U_2 d/I_x\\ U_3 d/I_y\\ U_4/I_z\end{bmatrix} \quad (26)$$

$$\begin{bmatrix}\dot{\phi}\\ \dot{\theta}\\ \dot{\psi}\end{bmatrix} = \begin{bmatrix}1 & sin(\phi)tan(\theta) & cos(\phi)tan(\theta)\\ 0 & cos(\phi) & -sin(\phi)\\ 0 & sin(\phi)/cos(\theta) & cos(\phi)/cos(\theta)\end{bmatrix}\begin{bmatrix}p\\ q\\ r\end{bmatrix} \quad (27)$$

Equation (25) is the final form of the nonlinear dynamic model for translational motion and equations (26), (27) are the final form of the nonlinear dynamic model for rotational motion.

D. The Simplified Nonlinear Dynamic Model

For translational dynamic model obtained in equation (25), simplification is not necessary. However, for rotational dynamics, transformation between $[\dot{p}, \dot{q}, \dot{r}]$ to $[\ddot{\phi}, \ddot{\theta}, \ddot{\psi}]$ is very complex since it involves so many trigonometric terms and derivatives. Therefore, to use in optimal control algorithm, rotational dynamic model will be simplified. The simplification is based on the assumption that if perturbations from hover condition are small, body angular rates $[p, q, r]$ and rate of change of Euler angles $[\dot{\phi}, \dot{\theta}, \dot{\psi}]$ can be taken as equal [3]. To clarify this assumption, tranformation matrix L_R defined in equation (16) can be examined. For small ϕ and θ, L_R can be taken as $I_{3\times3}$. Then, relation between body angular rates and rate of change of Euler angles becomes as follows:

$$\begin{bmatrix}p\\ q\\ r\end{bmatrix} = \begin{bmatrix}\dot{\phi}\\ \dot{\theta}\\ \dot{\psi}\end{bmatrix}, \quad \begin{bmatrix}\dot{p}\\ \dot{q}\\ \dot{r}\end{bmatrix} = \begin{bmatrix}\ddot{\phi}\\ \ddot{\theta}\\ \ddot{\psi}\end{bmatrix} \quad (28)$$

Then, substituting equation (28) into equation (26), the simplified nonlinear dynamic model for rotational motion is obtained as follows:

$$\begin{bmatrix}\ddot{\phi}\\ \ddot{\theta}\\ \ddot{\psi}\end{bmatrix} = \begin{bmatrix}(I_y - I_z)\dot{\theta}\dot{\psi}/I_x\\ (I_z - I_x)\dot{\phi}\dot{\psi}/I_y\\ (I_x - I_y)\dot{\phi}\dot{\theta}/I_z\end{bmatrix} + \begin{bmatrix}U_2 d/I_x\\ U_3 d/I_y\\ U_4/I_z\end{bmatrix} \quad (29)$$

As mentioned previously, the assumption made in this section is based on the fact that perturbations from hover condition are small. Therefore, in the optimal control algorithm, Euler angles ϕ and θ are constrained to get more reasonable results from simulations. It is important to note that simulations are performed by using the nonlinear dynamic model (non-simplified dynamic model) as plant.

According to the simulation results explained in section V, optimal control system works properly. Therefore, we can conclude that the assumption made in this section is reasonable.

Consequently, to use in optimal control algorithm, the simplified nonlinear dynamic model for translational and rotational motion are expressed in equations (25) and (29), respectively.

III. Linearization of The Simplified Nonlinear Dynamic Model

To use in discrete-time LQT algorithm (optimal control algorithm), the simplified nonlinear dynamic model has to be linearized around a trim condition.

First, state vector X, output vector Y and control vector U are defined in equation (30).

$$X = \begin{pmatrix}x_1\\ x_2\\ x_3\\ x_4\\ x_5\\ x_6\\ x_7\\ x_8\\ x_9\\ x_{10}\\ x_{11}\\ x_{12}\end{pmatrix} = \begin{pmatrix}\phi\\ \dot{\phi}\\ \theta\\ \dot{\theta}\\ \psi\\ \dot{\psi}\\ x\\ \dot{x}\\ y\\ \dot{y}\\ z\\ \dot{z}\end{pmatrix}, \quad Y = \begin{pmatrix}x_1\\ x_2\\ x_3\\ x_4\\ x_5\\ x_6\\ x_7\\ x_8\\ x_9\\ x_{10}\\ x_{11}\\ x_{12}\end{pmatrix}, \quad U = \begin{pmatrix}U_1\\ U_2\\ U_3\\ U_4\end{pmatrix} \quad (30)$$

Trim condition is chosen as hovering at an altitude of 1 meter. Then, at hover; $x_1 = x_2 = x_3 = x_4 = x_5 = x_6 = x_7 = x_8 = x_9 = x_{10} = x_{12} = 0$, only z coordinate, x_{11} = 1 meter.

Then, linearizing equations (25) and (29) around hover condition, equation (31) is obtained as a linearized state space system.

$$\dot{X} = AX + BU, \quad Y = CX \quad (31)$$

In equation (31), A, B and C are state, input and output matrices of the linearized state space system respectively. Linearized A, B and C matrices are found by using the "MATLAB Symbolic Toolbox".

IV. Discrete Time LQT Algorithm

A. Obtaining Discrete Time State Space Equations

First, continuous time linear state space system obtained in equation (31) has to be discretized. By choosing 0.01 seconds sample time, discrete-time state space system is obtained as equation (32).

$$X(k+1) = A_d X(k) + B_d U(k), \quad Y(k) = C_d X(k) \quad (32)$$

In equation (32), A_d, B_d and C_d are discrete-time state, input and output matrices respectively. "k" represents discrete time step i.e. $k = 1, 2, ..., k_f$, such that $k \in \mathbb{Z}^+$.

B. Selection of State Weight Matrix Q and Control Weight Matrix R

The performance index to be minimized J is defined in equation (33).

$$\begin{aligned} J = \frac{1}{2}[C_d X(k_f) - r(k_f)]^T F[C_d X(k_f) - r(k_f)] \\ + \frac{1}{2}\sum_{k=k_0}^{k_f-1}\Big([C_d X(k) - r(k)]^T Q[C_d X(k) - r(k)] + U^T(k) R U(k)\Big) \end{aligned} \tag{33}$$

Boundary condition $X(k_0) = X_0$ is the initial hover condition defined in section III.

The final state of the quadrotor at the end of the maneuver is set free. Therefore, $X(k_f)$ is free, k_f (final time) is fixed and F is 12×12 zero matrix for our case. $r(k)$ represents the desired state vector, in other words, desired trajectory to be followed, at time step k.

Q and R matrices are state weight matrix and control weight matrix respectively. The diagonal entries of Q matrix are chosen by trial and error such that good tracking performance is achieved while satisfying constraints on Euler angles defined in equation (35). The complete form of diagonal Q and R matrices are defined in the equation set (34). It is important to note that while comparing the optimal control system used in this paper with the fixed gain LQR control, the same Q and R matrices are used.

$$\left.\begin{aligned} Q = diag[100, 50, 10, 5, 0, 0, 100, 1, 100, 1, 1000, 0.1] \\ R = diag[10, 0, 0, 0] \end{aligned}\right\} \tag{34}$$

$$-20^\circ < \phi < 20^\circ, \;\; -20^\circ < \theta < 20^\circ, \;\; -20^\circ < \psi < 20^\circ \tag{35}$$

Satisfying constraints defined in equation (35) is not necessary but preferable since optimal control system is obtained by using the simplified and linearized model which is the approximation of the nonlinear dynamic model in the vicinity of the hover condition. Therefore, to get more accurate results from simulations which are performed by using the nonlinear dynamic model as plant, perturbations from hover condition should stay in the regions defined in equation (35).

Although, satisfying the constraints defined in equation (35) is preferable, simulation results of the disturbance rejection analysis show that optimal control system gives good tracking performance even for high Euler angles, up to 70°, as can be seen in Figure 22. This demonstrates that the modeling errors between the true nonlinear dynamics of the quadrotor and the simplified linear model are within the robustness levels of the optimal control system.

C. Optimal Control Algorithm

The equation set (36) is used to find the solution of discrete-time LQT control problem [2].

$$\left.\begin{aligned} P(k) = A_d^T P(k+1)[I + EP(k+1)]^{-1} A_d + V \\ V = C_d^T Q C_d \\ E = B_d R^{-1} B_d^T \\ g(k) = [A_d^T - A_d^T P(k+1)[I + EP(k+1)]^{-1} E] \\ g(k+1) + C^T Q r(k) \\ X^*(k+1) = [A_d - B_d L(k)] X^*(k) + \\ B_d L_g(k) g(k+1) \\ L(k) = [R + B_d^T P(k+1) B_d]^{-1} B_d P(k+1) A_d \\ L_g(k) = [R + B_d^T P(k+1) B_d]^{-1} B_d^T \\ U^*(k) = -L(k) X^*(k) + L_g(k) g(k+1) \end{aligned}\right\} \tag{36}$$

Boundary conditions at final time k_f are as follows:

$$\left.\begin{aligned} P(k_f) = C_d^T F C_d \\ g(k_f) = C_d^T F \; r(k_f) \end{aligned}\right\} \tag{37}$$

The first equation of the equation set (36) is the famous matrix difference Riccati Equation. The equation set (36) is integrated backwards in time to find the time-variant optimal control gains L, L_g and g, off-line. The boundary conditions defined in equation (37) are used as the starting point of integration. The size of L and L_g matrices are 4×12 and size of g matrix is 12×1.

Once the optimal control gains L, L_g and g are obtained off-line, these values are substituted into the last equation of equation set (36) to obtain optimal control inputs U^* at each time step k. Analyzing optimal control gains L, L_g and g showed that, L and L_g can be considered as time-invariant, approximately. However, it is observed that, g is time-variant and it varies in proportion to the desired trajetory to be followed. Therefore, we can conclude that the main difference between the LQT control used in this paper and the fixed gain LQR control is the time-variant optimal control gain g which is directly related to the desired trajectory.

Figure 2 shows the basic model of the optimal control system used in simulations. Green block represents the nonlinear dynamic model of the quadrotor obtained in equations (25), (26), (27) and yellow blocks represent time-variant optimal control gains L, L_g and g.

It is important to note that, simulation step size is variable; however, optimal control gains L, L_g and g are found by using fixed step size of 0.01 seconds. To solve this problem, interpolation is used to find the values of L, L_g and g at time steps which are not exact multiple of 0.01, for example at time step 0.0136 or 0.0292. Therefore, it can be said that solutions used in simulations are suboptimal. Actually,

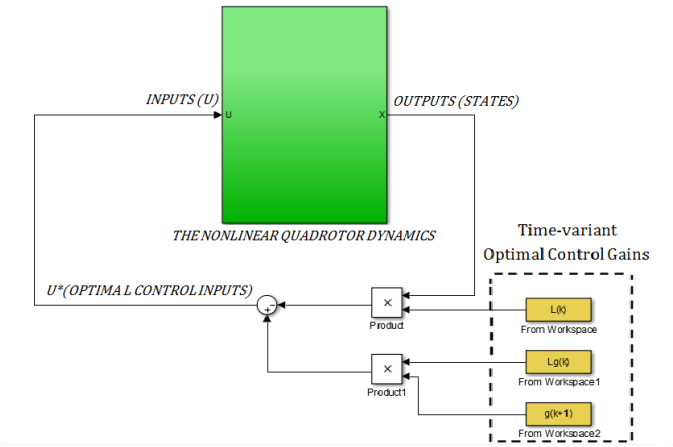

Fig. 2. The optimal control system as a state feedback control, green block is the nonlinear dynamic model and yellow blocks are time-variant optimal control gains

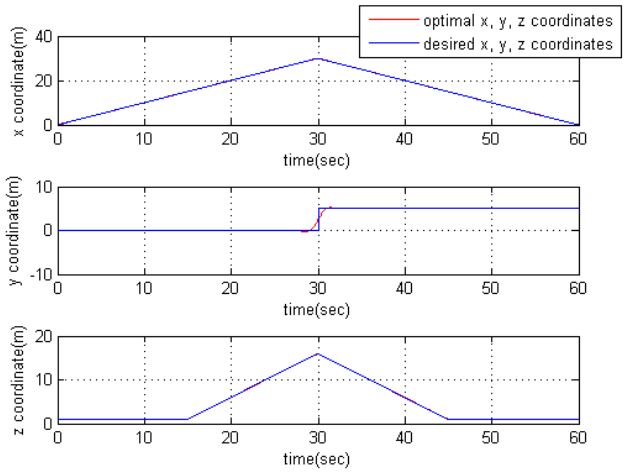

Fig. 3. Desired trajectory and optimal trajectory obtained for trajectory defined in subsection A

discretizing the system directly turns the optimal control solution into a suboptimal control solution.

V. Results and Discussion

A. Simple Trajectory That Involves Climb, Turn, Descent and Cruise Flight

For this trajectory, quadrotor is hovering at 1 meter initially. Then, it makes cruise flight until 15 seconds. At 15 seconds, quadrotor starts to climb until 30 seconds. At 30 seconds, a step input of 5 meter is given for y coordinate. At 30 seconds, quadrotor also starts to descent until 45 seconds. Between 45 seconds and 60 seconds, quadrotor makes cruise flight and stops at 60 seconds.

As can be seen in Figures 3 and 4, simulations give good tracking performance. Figure 4 shows that at steady states, maximum tracking error for translational motion is about 0.01 meter which is acceptable.

An interesting result of this case is as follows; as can be seen in Figure 5, a step input of 5 meter is given at 30 seconds for y coordinate, since optimal control gains are calculated off-line, quadrotor knowns that step command will be applied at 30 seconds, therefore it can react before 30 seconds. This result make sense because in LQT algorithm defined in equation (36), trajectory is defined at first and then the optimal control gains are calculated off-line. By this way, although a step command is given to the system, optimal control inputs U_1 and U_2 which are related to the motion in y direction, changes slowly and motors do not saturate due to sharp changes in U_1 and U_2. As can be seen in Figure 6, this result can't be obtained in fixed gain LQR control. Fixed-gain LQR control reacts to the step command applied at 30 seconds at that exact moment, not before 30 seconds. Therefore, we can conclude that for trajectories that involve sharp maneuvers or step commands, LQT control system used in this paper is advantageous to the fixed gain LQR control.

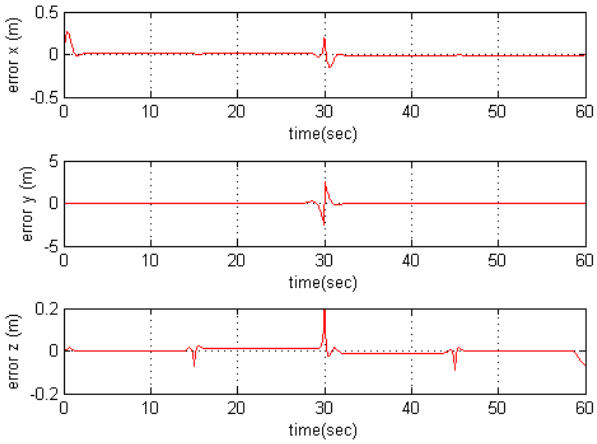

Fig. 4. Tracking errors for x, y, z coordinates for trajectory defined in subsection A

Figure 7 shows the optimal control input U_1 and weight of the quadrotor. It is seen that for cruise flight (0-15 seconds and 45-60 seconds) total force generated by four propellers, U_1 equals to 4.7099 N. This value is slightly greater than weight of the quadrotor which is 4.7088 N. In addition, for climb (15-30 seconds) U_1 is greater than weight and for descent (30-45 seconds) U_1 is less than weight, as expected. To compare the values of U_1 with the fixed gain LQR control we can analyze Figures 7 and 8. As can be seen in Figure 8, for fixed gain LQR control, maximum U_1 reaches about 7.5 N which is approximately 2 N greater than the LQT control used in this paper. According to these results, we can conclude that time-variant gain LQT control system is energy efficient compared to the fixed-gain LQR control especially for the trajectories that involve sharp maneuvers. It is important to remind that in comparisons, same state

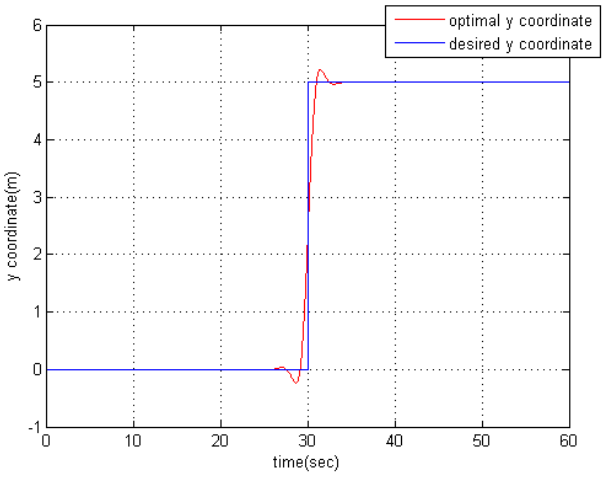

Fig. 5. For time-variant gain LQT control used in this paper, desired and optimal y coordinates obtained for trajectory defined in subsection A , it is seen that due to the nature of the optimal control algorithm, quadrotor can react before a step input is commanded at 30 seconds.

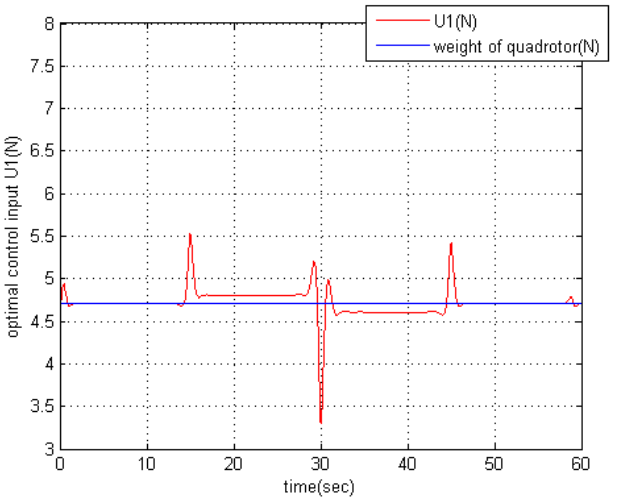

Fig. 7. For time-variant gain LQT control used in this paper, optimal control input U_1 for trajectory defined in subsection A

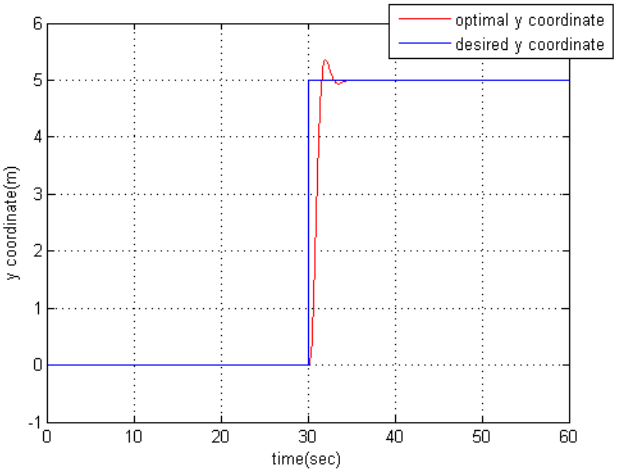

Fig. 6. For fixed gain LQR control, desired and optimal y coordinates obtained for trajectory defined in subsection A, it is seen that LQR control can not react before a step input is commanded at 30 seconds.

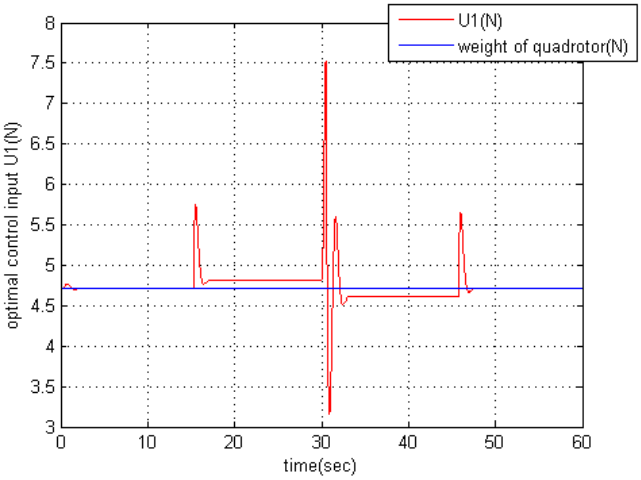

Fig. 8. For fixed gain LQR control, optimal control input U_1 for trajectory defined in subsection A

weight matrix Q and control weight matrix R are used for each control system.

The only aim is not decreasing energy consumption, there are also some constraints that should be satisfied for some states, i.e. Euler angles. Figure 9 shows the optimal Euler angles obtained for the time-variant gain LQT control system over the whole trajectory. It is seen that Euler angles stay in the limits between -20° and 20° which are defined in equation (35). These bounds for Euler angles should be satisfied, since optimal control algorithm is solved by using the linearization of the simplified nonlinear dynamic model which assumes that perturbations from hover condition are small. Therefore, to get more accurate results from simulations which are performed by using the nonlinear dynamic model as plant, staying in the vicinity of hover condition is beneficial. However, in disturbance rejection analysis, it is also observed that, optimal control systems works well for Euler angles, up to 70°. This result shows that optimal control system is also valid for high Euler angles.

As can be seen in Figure (10), optimal Euler angles for fixed gain LQR control reaches up to 50°, although the values for LQT control used in this paper are 20° maximum, according to Figure (9). This is due to the fact that LQR control can not react to the step command before it is applied at 30 seconds, as LQT control system used in this paper. By this way, LQT control can handle sharp maneuver commanded at 30 seconds with lower Euler angles, in other words, more smoothly which can be seen in Figure 9.

Moreover, Figure 11 shows the optimal states for $\dot{x}$,$\dot{y}$,

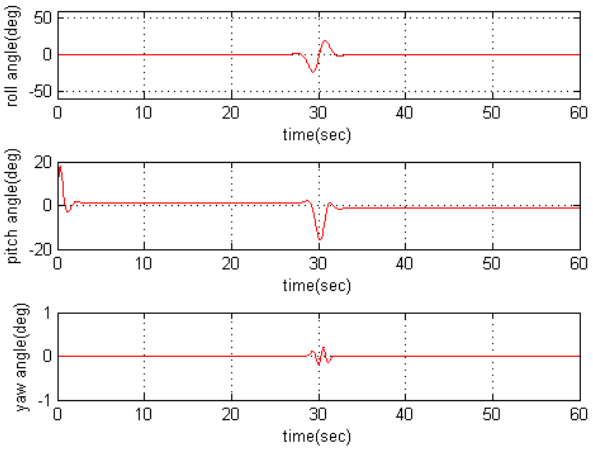

Fig. 9. For time-variant gain LQT control used in this paper, optimal Euler angles obtained for trajectory defined in subsection A

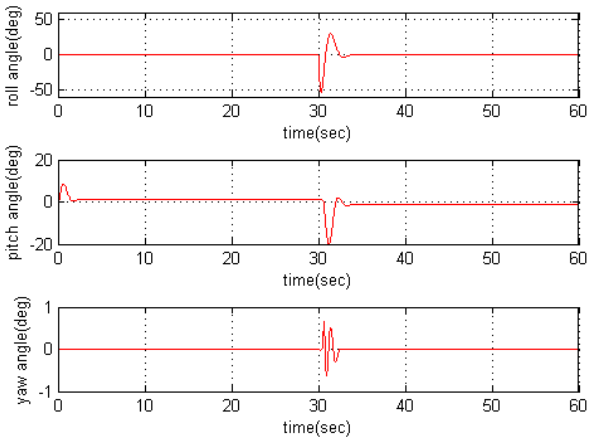

Fig. 10. For fixed gain LQR control, optimal Euler angles obtained for trajectory defined in subsection A

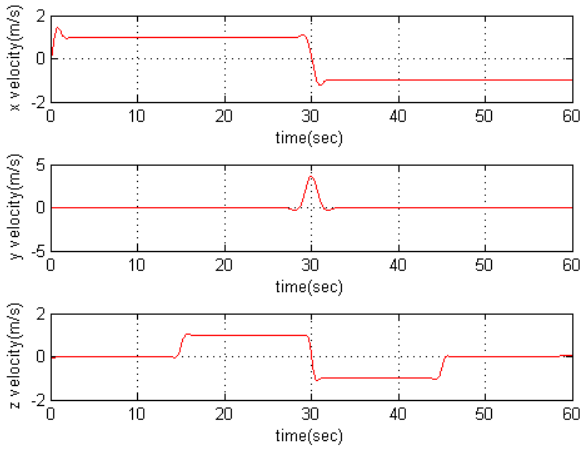

Fig. 11. Optimal translational velocities obtained for trajectory defined in subsection A

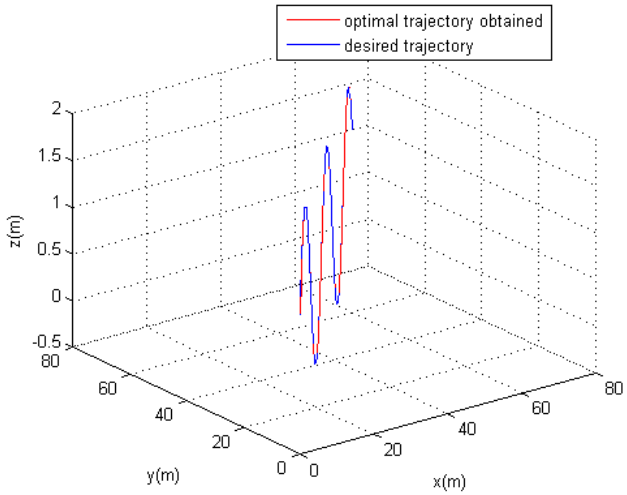

Fig. 12. Desired trajectory and optimal trajectory obtained for trajectory defined in subsection B

$\dot{z}$, in other words, translational velocities. Results are physically realistic and reasonable for the trajectory defined in subsection A.

B. A more complex trajectory

In this case, a more complex trajectory which involves sinusoidal climb and descent is defined as desired trajectory.

As can be seen in Figures 12 and 13, we can conclude that desired trajectory is followed accurately. According to Figure 13, maximum tracking error for translational states at steady state is about 0.01 meter which is acceptable.

Figure 14 shows the optimal control input U_1 and weight of the quadrotor. As can be seen in Figure 14, U_1 is controlled optimally to decrease energy consumption.

As can be seen in Figure 15, Euler angles stay in the regions defined in equation (35). Moreover, according to Figure 16, it is seen that translational velocities $\dot{x}$, $\dot{y}$, $\dot{z}$ are physically reasonable.

Some other complex paths are also tested and it is seen that simulations give accurate tracking performance while decreasing energy consumption by controlling U_1 optimally.

C. Disturbance Rejection

In this section disturbance rejection properties of the optimal control system will be analyzed. First, the nonlinear dynamic model for translational motion obtained in equation (23) will be rewritten as following:

$$\begin{bmatrix} \sum F_{ext,x} \\ \sum F_{ext,y} \\ \sum F_{ext,z} \end{bmatrix} = -L_{BE}\, m \begin{bmatrix} 0 \\ 0 \\ g \end{bmatrix} + \begin{bmatrix} 0 \\ 0 \\ U_1 \end{bmatrix} - K_t V_B + \begin{bmatrix} D_x \\ D_y \\ D_z \end{bmatrix} \quad (38)$$

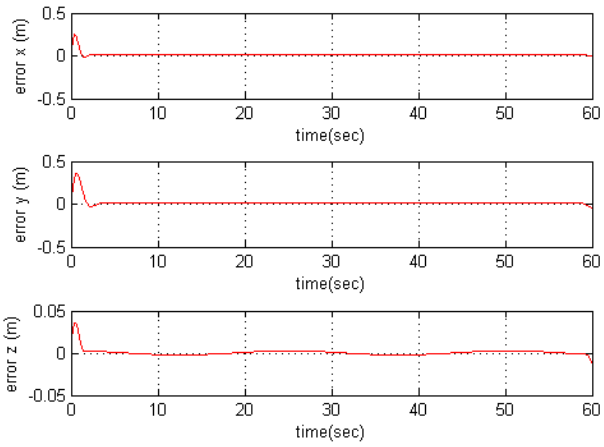

Fig. 13. Tracking errors for x, y, z coordinates for trajectory defined in subsection B

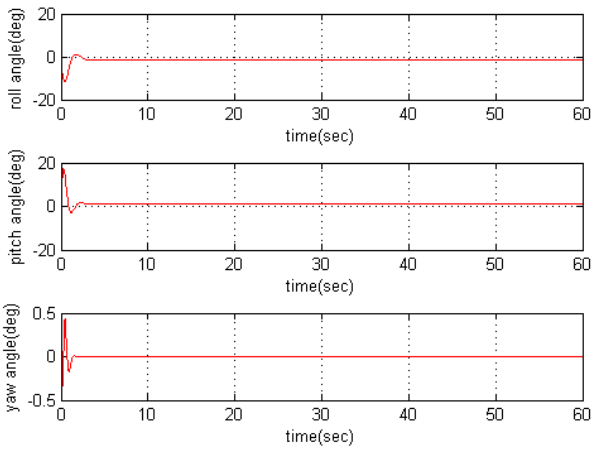

Fig. 15. Optimal Euler angles obtained for trajectory defined in subsection B

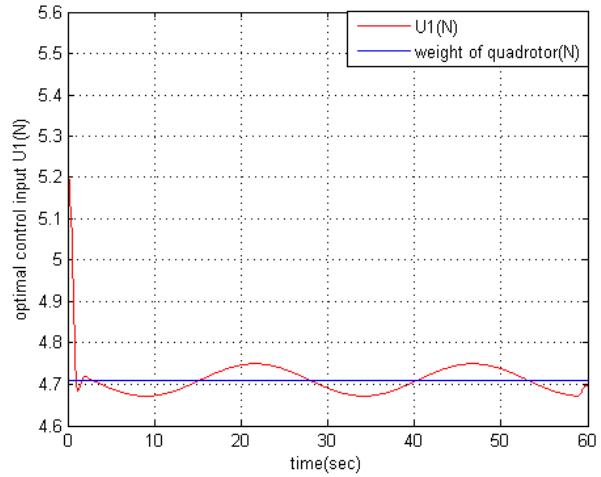

Fig. 14. Optimal control input U_1 for trajectory defined in subsection B

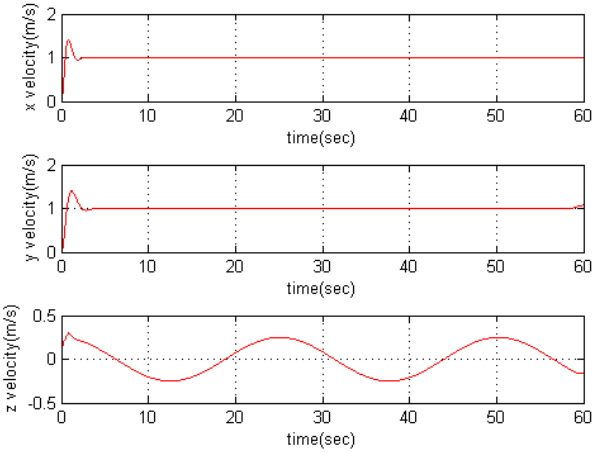

Fig. 16. Optimal translational velocities obtained for trajectory defined in subsection B

where D_x, D_y, D_z represent additional disturbance terms. As can be seen in equation (38), disturbances are added to the system as additional external forces, therefore they are in the units of [N].

Figures 17, 18, 19 shows the numerical values of $\sum F_{ext,x}$, $\sum F_{ext,y}$ and $\sum F_{ext,z}$ with disturbances added to the system, respectively.

As can be seen in Figures 17 and 18, for the motion in x and y direction, a strong constant disturbance is added to system at 5 and 10 seconds, respectively. Since constant disturbances are very strong, they last for 0.2 seconds, therefore they can be considered as impulse disturbances. Moreover, according to Figure 19, for the motion in z direction, a Gaussian distributed random disturbance is added to the system between 15 to 25 seconds. Mean and variance of the Gaussian distribution are 0 and 1 respectively. As can be seen in Figures 17, 18 and 19, all of the disturbances are added simultaneously.

For the disturbance rejection analysis, trajectory defined in subsection B will be used as desired trajectory. Only difference is that the simulations are performed for 30 seconds to see the effects of disturbances more clearly.

As can be seen in Figures 20 and 21, disturbances are successfully rejected. At 5 and 10 seconds, quadrotor is exposed to strong impulse disturbances and deviate from the desired path. However, as can be seen in Figure 22, optimal control system try to return to the desired path by changing Euler angles significantly.

An important result is that, according to the Figure 22, to reject disturbances rapidly, Euler angles can reach up to 70°. As mentioned previously, optimal control system is obtained by using linearized model which is the approximation of the simplified nonlinear dynamic model if perturbations from

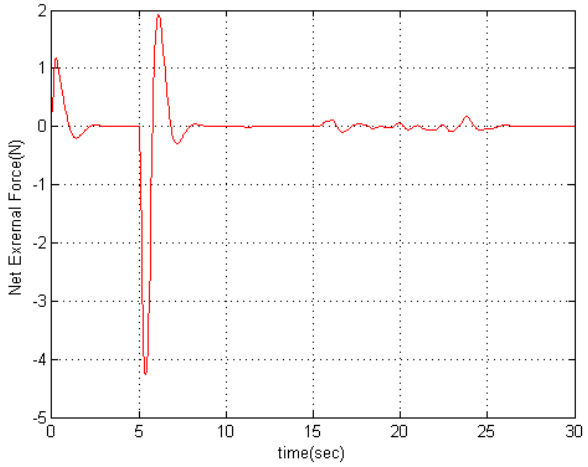

Fig. 17. $\sum F_{ext,x}$ defined in equation (38) with a strong impulse disturbance added at 5 seconds

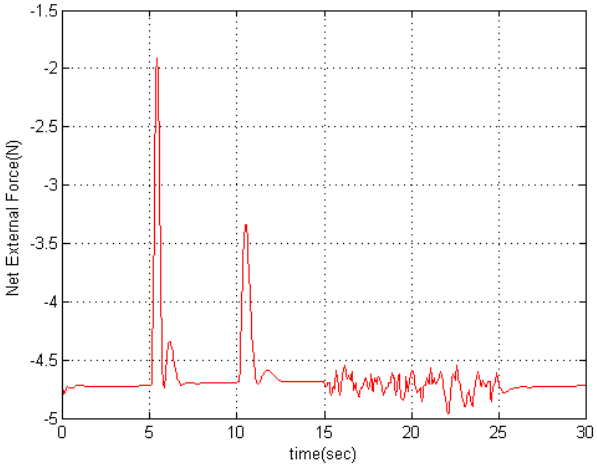

Fig. 19. $\sum F_{ext,z}$ defined in equation (38) with a Gaussian distributed disturbance added between 15 to 25 seconds

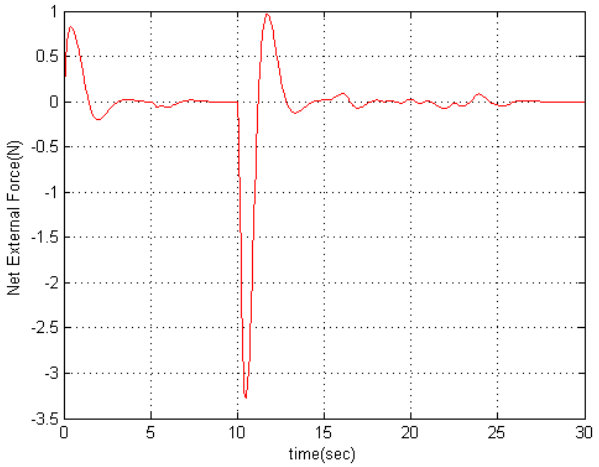

Fig. 18. $\sum F_{ext,y}$ defined in equation (38) with a strong impulse disturbance added at 10 seconds

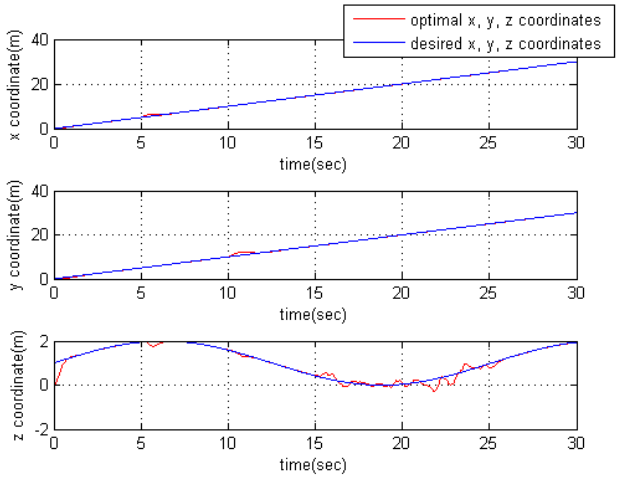

Fig. 20. Desired and optimal trajectory obtained with disturbances added to the system

hover condition are small. Therefore, some constraints were defined in equation (35) to stay close to the hover condition. Nevertheless, according to Figure 22, we can conclude that, optimal control system works well even for high Euler angles, up to 70°. This result motivates to test the optimal control system for the trajectories that involve very high maneuverability.

VI. Conclusion

In this paper, a discrete time LQT controller is designed for optimal path tracking of a quadrotor. Instead of using common LQR control with fixed control gains, time variant optimal control gains are used. First, the nonlinear dynamic model of the quadrotor is obtained by using Newton's equations of motion. Then, this model is simplified, linearized and discretized to use in the optimal control algorithm. Time-variant optimal control gains are found off-line by solving discrete matrix difference Riccati Equation backwards in time. Finally, optimal control system is simulated by using the nonlinear dynamic model as plant and optimal control gains as state feedback. In addition, disturbance rejection properties of the optimal control system are tested by simulations.

Simulations show that, good tracking performance is achieved while decreasing energy consumption compared to the fixed gain LQR control. The motivation of this study was decreasing high energy consumption which is one of the main disadvantages of quadrotor UAVs. By using the optimal control method defined in this paper, energy consumption can be decreased reasonably especially for trajectories that involve high maneuvers.

Some other advantageous properties of the optimal control

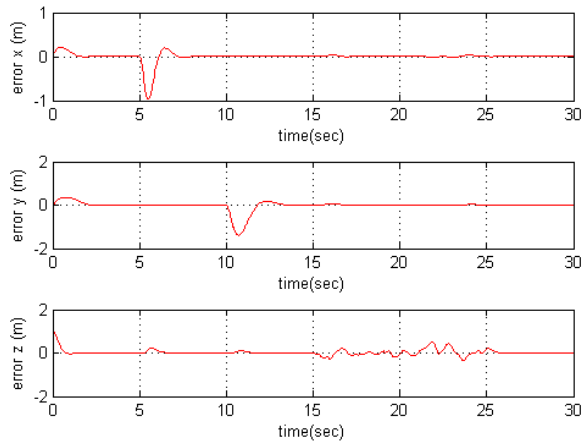

Fig. 21. Tracking errors for x, y, z coordinates with disturbances added to the system

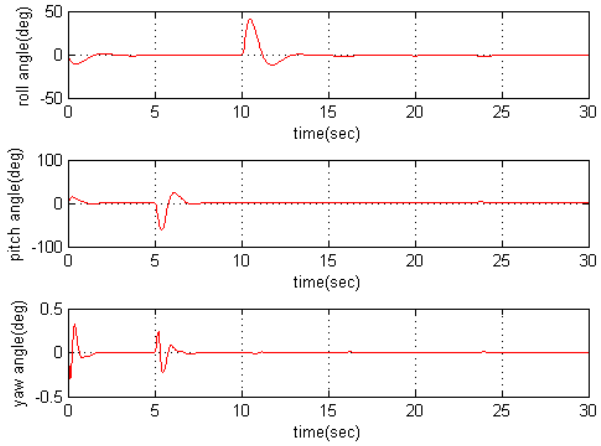

Fig. 22. Optimal Euler angles with disturbances added to the system

system used in this paper compared to the fixed gain LQR control are also analyzed. In a future study, a more detailed comparison analysis can be made.

To extend the study, some terms that are neglected in the derivation of quadrotor's dynamic model can be added to the dynamic model and a more accurate drag model can be used for control system design and simulations.

The positive results obtained in simulations encourage to validate the optimal control system by making real time experiments in future.

REFERENCES

[1] R. Xu and U. Ozguner, "Sliding mode control of a quadrotor helicopter", *Proceedings of the IEEE 45th Conference on Decision & Control*, San Diego, CA, USA, December 2006, pp. 4957-4962.

[2] D. S. Naidu, *Optimal Control Systems*, CRC Press LLC, Florida, USA, 2003.

[3] S. Bouabdallah, "Design and control of quadrotors with application to autonomous flying", Ph.D. thesis, Ecole Polytechnique Federale de Lausanne, Lausanne, France, 2007.

[4] S. H. Lee, S. H. Kang and Y. Kim, "Trajectory tracking control of Quadrotor UAV", *Proceedings of the ICCAS International Conference on Control, Automation and Systems*, Gyeonggi-do, Korea, October 2011, pp. 281-285.

[5] S. Bouabdallah and R. Siegwart, "Backstepping and sliding-mode techniques applied to an indoor micro quadrotor", *Proceedings of the IEEE International Conference on Robotics and Automation*, Barcelona, Spain, April 2005, pp. 2247-2252.

[6] M. Achtelik, "Nonlinear and adaptive control of a quadcopter", Dipl.-Ing. Dissertation, Lehrstuhl fr Flugsystemdynamik, Technische Universitt Mnchen, Garching, Germany, 2010.

[7] Y. M. Al-Younes, M. A. Al-Jarrah and A. A. Jhemi, "Linear vs. nonlinear control techniques for a quadrotor vehicle", *Proceedings of the ISMA10 International Symposium on Mechatronics and its Applications*, Sharjah, UAE, April 2010, pp. 1-10.

[8] D. Lee, C. Nataraj, T. C. Burg and D. M. Dawson, "Adaptive tracking control of an underactuated aerial vehicle", *Proceedings of the American Control Conference*, San Francisco, CA, USA, June-July 2011, pp. 2326-2331.

[9] J. Berg, D. Wilkie, S. J. Guy, M. Niethammer and D. Manocha, "LQG-obstacles: Feedback control with collision avoidance for mobile robots with motion and sensing uncertainty", *Proceedings of the IEEE International Conference on Robotics and Automation*, Saint Paul, Minnesota, USA, May 2012, pp. 346-353.

[10] T. Madani and A. Benallegue, "Backstepping control for a quadrotor helicopter", *Proceedings of the IEEE/RSJ International Conference on Intelligent Robots and Systems*, Beijing, China, October 2006, pp. 3255-3260.

[11] Y. Li and S. Song, "A survey of control algorithms for quadrotor unmanned helicopter", *Proceedings of the IEEE fifth International Conference on Advanced Computational Intelligence(ICACI)*, Nanjing, Jiangsu, China, October 2012, pp. 365-369.

[12] B. Panomrattanarug, K. Higuchi and F. Mora-Camino, "Attitude control of a quadrotor aircraft using LQR state feedback controller with full order state observer", *Proceedings of the SICE Annual Conference 2013*, Nagoya, Japan, September 2013, pp. 2041-2046.

[13] B. Etkin, *Dynamics of Atmospheric Flight*, Dover Publications, New York, USA, 2005.

[14] A. A. Shabana, *Dynamics of Multibody Systems*, Cambridge University Press, New York, USA, 2005.

[15] G. D. Padfield, *Helicopter Flight Dynamics: The Theory and Application of Flying Qualities and Simulation Modelling*, Blackwell Publishing, Washington DC, USA, 2007.